Complex structure of the lithospheric slab beneath the Banda arc, eastern Indonesia depicted by a seismic tomographic model

Sri Widiyantoro,[1] Jeremy D. Pesicek,[2] Clifford H. Thurber[2]

[1]Faculty of Mining and Petroleum Engineering, Bandung Institute of Technology, Bandung, Indonesia; [2]Department of Geoscience, University of Wisconsin-Madison, Madison WI, USA

Abstract

Seismic tomography with a non-linear approach has been successfully applied to image the P-wave velocity structure beneath the Banda arc in detail. Nearly one million compressional phases including the surface-reflected depth phases pP and pwP from events within the Indonesian region have been used. The depth phases have been incorporated in order to improve the sampling of the upper-mantle structure, particularly below the Banda Sea in the back-arc regions. For the model parameterization, we have combined a high-resolution regional inversion with a low-resolution global inversion to allow detailed images of slab structures within the study region and to minimize the mapping of distant aspherical mantle structure into the volume under study. In this paper, we focus our discussion on the upper mantle and transition zone structure beneath the curved Banda arc. The tomographic images confirm previous observations of the twisting of the slab in the upper mantle, forming a spoon-shaped structure beneath the Banda arc. A slab lying flat on the 660 km discontinuity beneath the Banda Sea is also well imaged. Further interpretations of the resulting tomograms and seismicity data support the scenario of the Banda arc subduction rollback.

Introduction

The tectonic setting of the Indonesian archipelago in southeastern Eurasia is determined by the complex interaction of several major and minor plates. The junction of island arcs includes the Sunda arc, the Banda arc, the Molucca Collision Zone, and western Papua (New Guinea). This study is focused on the Banda arc that displays a strong curvature in map view.

Katili[1] reported that the strike of the Banda arc formerly was east-west, just like the eastern part of the Sunda arc, but it was twisted counter-clockwise in the Pliocene due to the combination of the collision with the northward moving Australian continent, the counter-clockwise rotation of the Bird's Head of New Guinea, and the westward movement of the Pacific. These tectonic events interrupted the regular growth of the eastern Indonesian arc. The report by Katili[1] supports the previous work by Hatherton and Dickinson,[2] who show a 180° bend of the slab inferred from the hypocenter depth contours. On the other hand, Fitch and Hamilton[3] show only a nearly 90° bend at the eastern end of the Banda arc. Cardwell and Isacks[4] conducted a detailed study of the spatial distribution of carefully relocated events and fault plane solutions in eastern Indonesia. They found that the data do not require a continuous 180° bend of the slab, but are best modeled by two subduction zones along the southern and northern parts (arms) of the Banda arc, decoupled by the Tarera Audina fault at the eastern end of the Banda arc (Figure 1). A decade later, McCaffrey[5] studied the active tectonics of the eastern Sunda and Banda arcs by using depths and fault plane solutions of large earthquakes. Intriguingly, he observed that the closure of the Banda basin (within the Banda arc) is geometrically incompatible with the Australian continental plate subducting beneath both the southern and northern arms of the Banda arc simultaneously. Instead, the Bird's Head subducting beneath the Seram trough is decoupled from the Australian plate. Matejkova *et al*.[6] bring seismological arguments also in favor of a two-slab model of the Banda arc region. They studied the region by using an updated version of the high quality hypocentral data set by Engdahl *et al*.[7] and global CMT solutions. Two oppositely dipping subduction zones are well discriminated by the seismicity data.

Focal mechanisms of events in the Banda region depict generally normal and reverse types with non-uniform orientation of nodal planes and stress axes.[6] Given this complex tectonic setting, it can be expected that the Banda arc overlies a strongly heterogeneous mantle. This structural complexity is partly evident from the seismicity. From seismic tomography, Puspito *et al.*,[8] Widiyantoro and van der Hilst,[9] and Bijwaard *et al.*[10] confirm the existence of the twisting of the slab beneath the Banda arc. Recently, Spakman and Hall[11] combined seismic tomography with the plate tectonic evolution of the Banda region and proposed a very interesting scenario, *i.e*., the Banda arc results from subduction rollback of a single slab. The aim of this study is to further explore the complex structure of lithospheric slab beneath the Banda arc by means of a seismic tomographic model derived using a non-linear approach[12] in order to clarify the contrasting explanations regarding the formation of the Banda arc, i.e., deformation of a single slab or two separate slabs subducting from the south and north.

Correspondence: Sri Widiyantoro, Faculty of Mining and Petroleum Engineering, Bandung Institute of Technology, Jl. Ganesha 10, Bandung 40132, Indonesia. E-mail: sriwid@geoph.itb.ac.id

Key words: Banda arc, non-linear seismic tomography, P-wave, subduction rollback, spoon-shape slab.

Acknowledgments: the authors would like to thank E. R. Engdahl, R. D. van der Hilst and R. Buland for the updated hypocentre and phase data set used in this study. This material is based upon work supported in part by NASA, under award NNX06AF10G. S. W. would like to thank the Institute of Technology Bandung (ITB) for the research grant (2010-2011) to conduct research on the seismotectonics of the Banda arc.

Received for publication: 15 June 2011.
Accepted for publication: 3 October 2011.

Research in Geophysics 2011; 1:e1
doi:10.4081/rg.2011.e1

Tomography with a non-linear approach

In this section we describe briefly the tomographic method using a non-linear approach applied in this study and the resolution tests used to assess image quality. We have used a cellular representation of mantle structure by discretizing the entire mantle using cells of 5°×5° (with 16 layers down to the bottom of the mantle), but in the study region we have employed a finer grid of 0.5°×0.5° (with 19 layers down to 1600 km) in order to allow the resolution of relatively small-scale structures. Such a model parameterization minimizes contamination by structures outside the volume being investigated.[9,13,14] We solved for perturbations to 178,272 model slowness cells using the iterative LSQR algorithm,[15] a conjugate gradient technique first used in seismic tomography by Nolet.[16] Following Bijwaard and Spakman[17] and Widiyantoro *et al*.,[18] we used a step-wise procedure to solve the non-linear travel-time inversion for seismic velocity variations. In the main step, ray paths and travel times are updated by 3-D ray tracing through intermediate realizations of the model. The 3-D ray tracing is based on the pseudo-bending method of Koketsu and Sekine,[19] originally

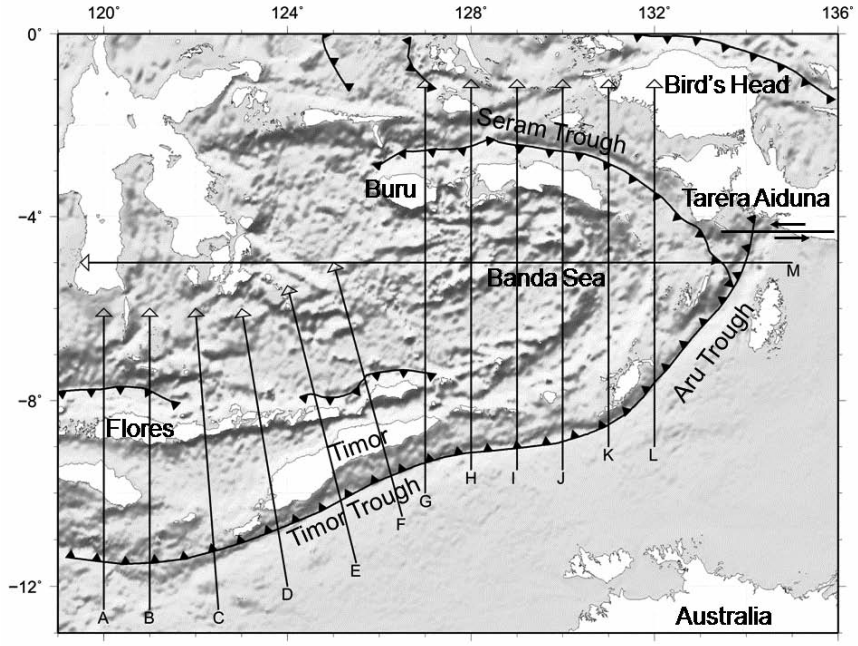

Figure 1. Map of the study region. Black lines indicate the position of the vertical cross sections displayed in Figure 4.

developed by Um and Thurber.[20] In the study by Pesicek *et al.*,[12] this procedure was improved by the use of an a priori global crustal model (CRUST 2.0)[21] in order to reduce the effect of the crust, which will generally not be resolved, on the imaging of the deeper structure.[22] In the Indonesian region, we initially traced rays from stations to sources through the global spherically symmetric model ak135[23] with the shallowest layer modified by the *a priori* crustal model. Iteratively Reweighted Least Squares, an approximation to the L1 norm solution,[24] was used to yield a more robust inversion less sensitive to data outliers. We remark that the images produced by this non-linear inversion are comparable to those of a one-step linearization, but the progressive updating of the slowness field, earthquake locations, and ray paths results in larger amplitudes of the velocity perturbations of ~30%, which absolutely cannot be achieved via a single Least Squares iteration using lower damping.

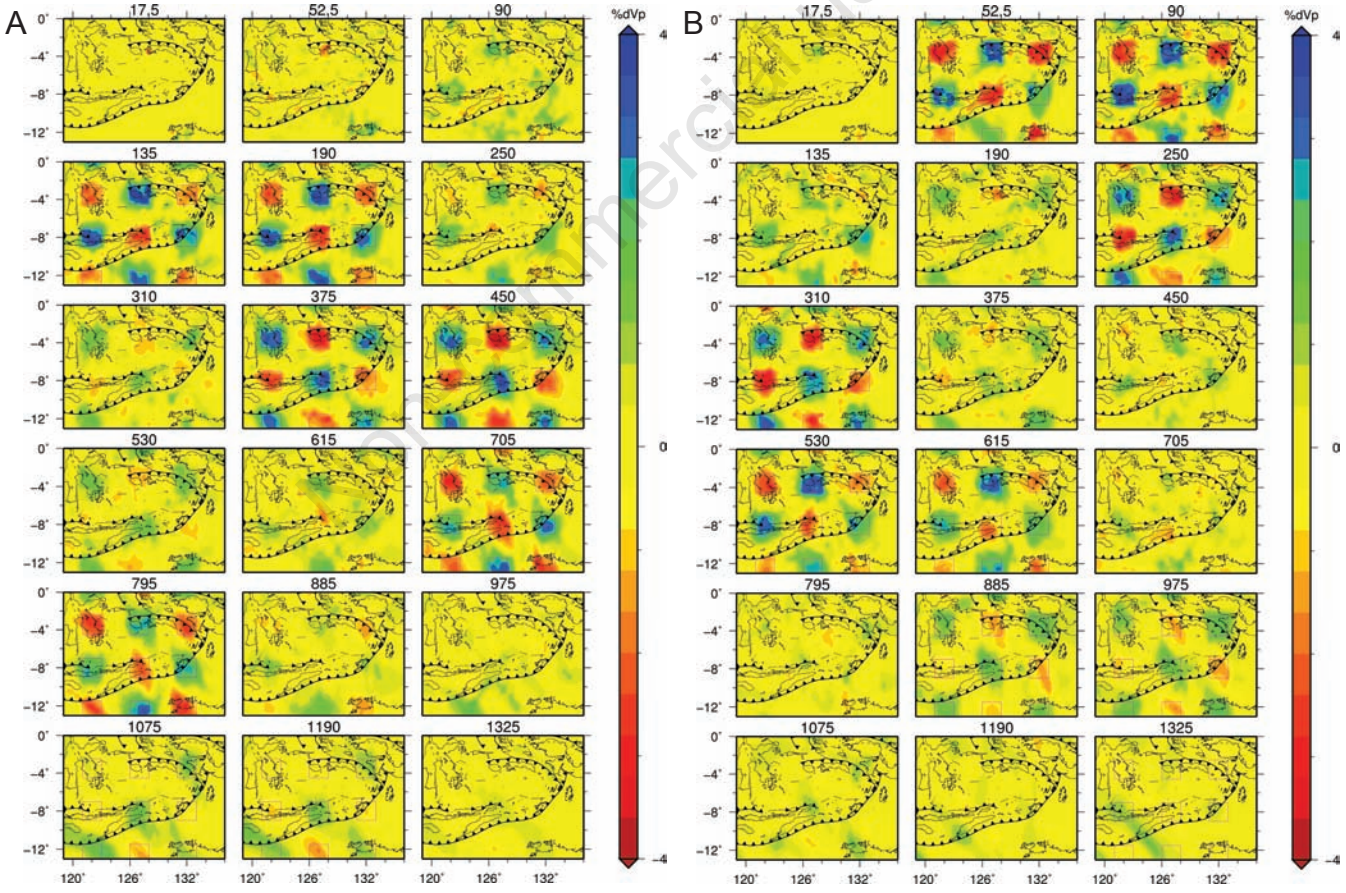

Figure 2. Resolution tests calculated using the same parameters as the real data inversion. A) Checkerboard model resolution tests after two iterations. Synthetic 4% velocity perturbation input checkerboard anomalies (2.5° x 2.5°; magenta contours) are separated by 2.5° in latitude and longitude and by 2 layers in depth. Depths with no input anomalies are shown and the perturbations in these layers are an indication of vertical smearing. B) Alternate checkerboard model, the same as (a) except the input pattern is shifted to be the opposite of (a), i.e. layers with (without) anomalies in (a) now lack (have) them.

Resolution tests using checkerboard anomaly models

We have assessed the tomographic images by conducting inversions of synthetic data computed from artificial but known 3-D models using the same ray coverage and non-linear approach used in the real data inversion. We have conducted inversions of synthetic data computed using two checkerboard anomaly models (Figure 2) with noise added. To simulate a more realistic distribution of noise, we randomized the actual residuals from the real inversion and added them to the synthetic data. We inverted the noisy synthetic data using damping parameters used in the real data inversion to see how well the shape of the input model and the amplitude are recovered. We have tuned the inversion by exploring the damping parameters that give the optimum trade off between bias (i.e., the amplitude recovery and smoothness in the model) and the variance reduction of the data.

Hypocentre and phase data set

In this study, we have used the updated hypocentre and phase data set of Engdahl, van der Hilst, and Buland (EHB)[7,25] covering the period 1964 to 2007. Previously, Engdahl *et al.*[7] carefully relocated nearly 100,000 earthquakes that occurred between 1964 and 1995 by using a nonlinear scheme and the radially stratified ak135 velocity model developed by Kennett *et al.*[23] These data consist of ~13 million P, pP, pwP, PKP, and S phase arrival times reported by almost 6000 globally distributed seismographic stations. The updated dataset used in this study consists of 957,262 compressional phases from events within the Indonesia region, including 10,640 pP and 4,239 pwP phases resulting from rather strict data selection criteria. A secondary azimuthal gap <180° was applied and only events with sufficient depth control (e.g. located using later arriving phases in addition to first arrivals) were used.

Presentation of the new tomographic images

P-wave travel-time residuals have been modeled in terms of velocity perturbations relative to the ak135 reference velocity model.[23] In this section we present the images achieved after conducting five iterations to update the 3-D velocity model. We note that the model presented here has no relocation between iterations. We present anomaly maps for depth intervals representing the upper mantle, transition zone and lower mantle (Figure 3). In order to illustrate the lateral variation in slab structure, vertical slices are also presented in detail (Figure 4).

From our inversions, we infer that the lithospheric slab is defined by a laterally continuous region of higher-than-average P-wave velocity in the mantle. The top layer anomaly map has had a crustal correction applied using the global crustal model CRUST 2.0[21] in the study region. The inversions reveal the twisting of the slab in the upper mantle, *i.e.,* from 90 to 190 km depth, which evidently parallels the present-day curved Banda arc (Figure 3). The strong low velocity anomalies in the uppermost mantle beneath the Banda Sea are in good agreement with the S wave speed structure derived from full waveform tomography by Fichtner *et al.*,[26] which has good resolution for structures in the upper mantle. Resolution tests indicate that sampling by seismic rays is sufficient to recover slab structure beneath the Banda region, in particular along the arc (Figure 2). In the mantle transition zone (530-615 km) the broadening in map view of the slab beneath the Banda Sea is clearly imaged and also resolved.

The complex lateral variation in slab structure beneath the Banda arc is further illustrated by vertical sections across the arc (Figure 4). The images in Figure 4 suggest that the Indo-Australian plate dips steeply beneath Flores and Timor (cross sections A – F) and is also well outlined by a seismic zone. Intriguingly, the images depict a slab lying flat in the mantle transition zone that extends to below the Timor trough, which is resolved by

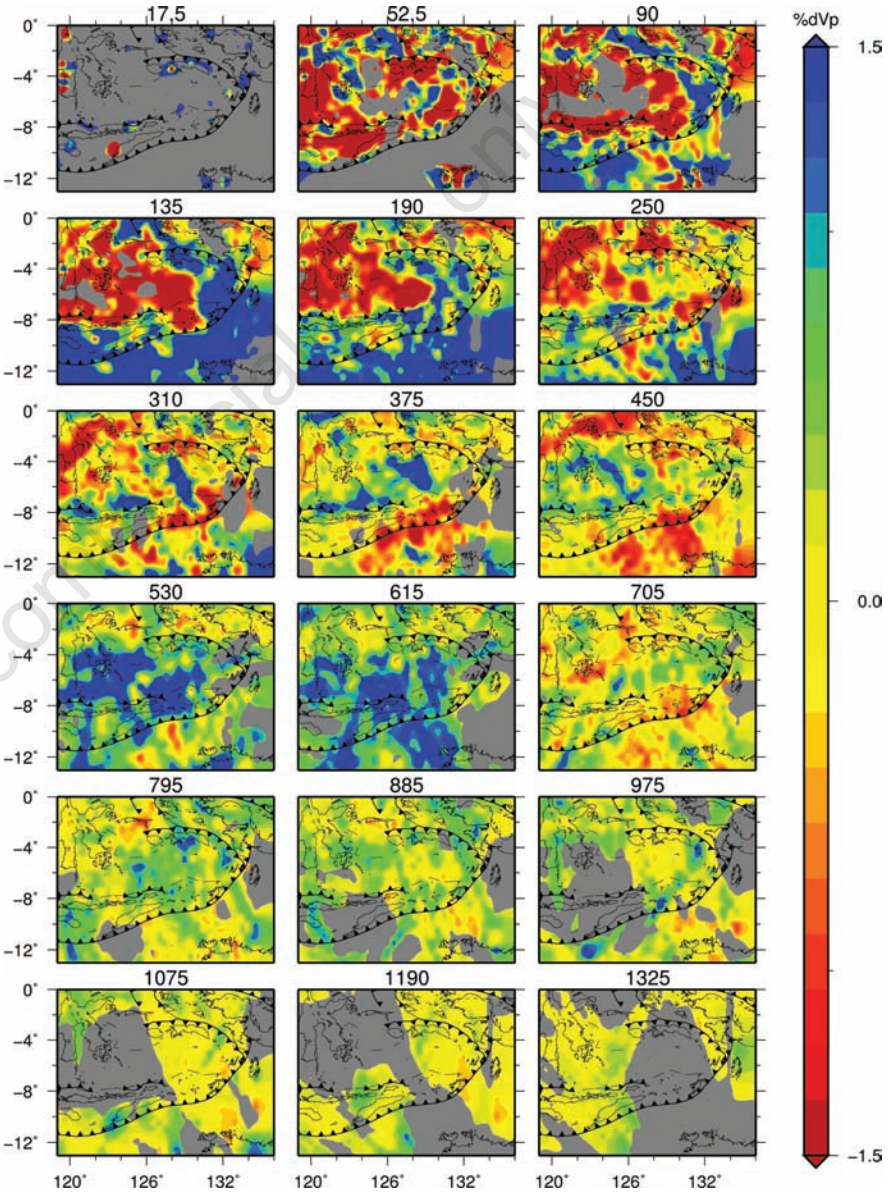

Figure 3. Layer anomaly maps depicting results of the inversion using full P-wave arrival time data for upper-mantle, transition zone and lower mantle structures below the Banda arc. Velocity perturbations relative to ak135 developed by Kennett *et al.*[23] are shown from –1.5% to +1.5%. For each map, mid-layer depths are listed in km at the top. Grey depicts mantle regions of poor sampling.

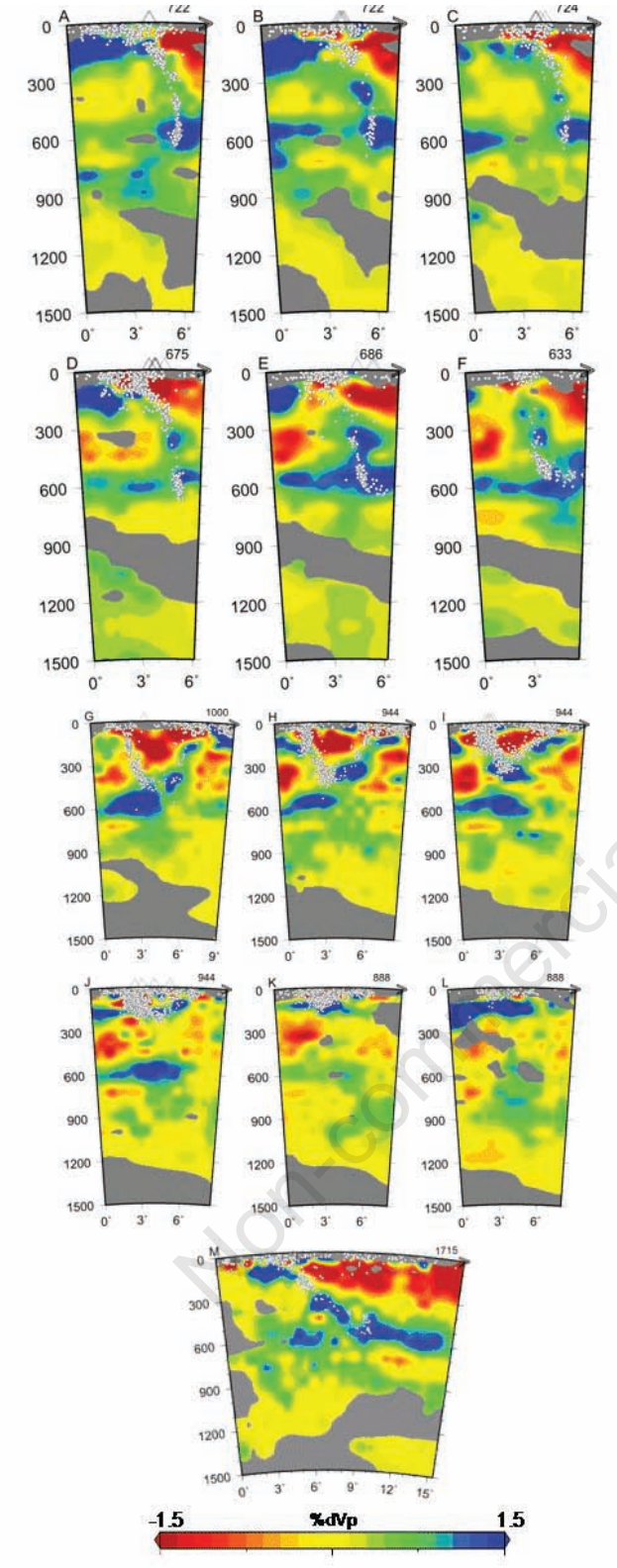

Figure 4. Vertical sections across the convergent margin in the contorted Banda arc through the P-wave model plotted as velocity perturbations relative to ak135. Vertical sections A-F are around the Timor trough. Vertical sections G-L are across the southern (Aru trough) and northern (Seram trough) arms of the Banda arc; while M trending east-west depicts the deflected slab in the mantle transition zone. Contour scales are from -1.5% to +1.5%. Circles depict earthquake hypocenters projected from a distance of up to 55 km on both sides of the plane of section. For each region, the cross section length is listed at the top-right in km, and in degrees at the bottom-right. Grey depicts mantle regions of poor sampling.

the data coverage (Figure 2B). Further east, the images show northward and southward dipping slabs beneath the Aru and Seram troughs (cross sections G – L). The bottoming depth of the spoon shape of the slabs decreases rapidly eastward in excellent agreement with the seismicity and the tomographic model presented by Spakman and Hall.[11] The slab detachment beneath Buru as discussed in detail[11] is also confirmed by our model (see cross section G).

The seismic tomogram (cross section M) displayed in Figure 4 is shown to provide strong evidence for the slab deflection in the mantle transition zone beneath the Banda Sea. In the E-W direction, it is depicted clearly that the dip of the lithospheric slab is significantly gentler than those in the N-S direction. This gentle dip may be associated with the eastward migration of the eastern part of the Banda arc as reported by McCaffrey.[5]

Discussion and Conclusions

The seismic tomographic images reveal mantle structure beneath the Banda arc in detail. Some efforts for image enhancement have been conducted through the combination of the use of better data (extensively processed EHB data), the inclusion of a global inversion in the regional study, the use of depth phases, and the use of the non-linear approach. In the main step ray paths and travel times are updated by 3-D ray tracing through intermediate realizations of the model that minimizes the dependency on the reference 1-D velocity model used (compared to a one-step linearization).[27] The results of resolution tests suggest that the slab structure beneath the Banda arc is adequately resolved by the P-wave data. The new tomographic images depict the twisting of the slab in the upper mantle beneath the Banda arc. The complete exploration of the lateral variation in the shape of the subducted slab based on our tomography images (Figure 4) confirms that the large-scale structure of the slab in the upper mantle and transition zone beneath Banda forms a spoon-shaped feature.[4,9,28] Here, we note that the dominant blue in the transition zone (530 and 615 km depth as seen in Figure 3), which is interpreted as the flat slab, to some extent can be due to an inappropriate reference model, in which the reference velocity model may be rather too slow for the mantle transition region in the study area. However, the plots of seismicity (see cross sections E and F in Figure 4) support the deflection of the subducted slab in the mantle transition zone.

Regarding the formation of the Banda arc with its spoon shape, there have been two contrasting explanations: i) the deformation of a

single slab, and ii) the two separate slabs subducting from the south and north. The explanation of the deformation of a single slab has been based mainly on seismicity data i.e. the hypocenter depth contours.[2] However, there is a seismicity gap underneath the eastern Banda arc, separating the laterally continuous seismicity zones beneath the Aru and Seram troughs. This supports the interpretation that the rotation of the arc is 90° as proposed by Fitch and Hamilton[3] and not 180°. It is rather difficult to envisage that a full 180° rotation of such a long arc (about 1200 km) can occur without any disruption. Furthermore, our seismic tomographic images do not show a long slab in the mantle trending east-west, which might have been important evidence to explain the full 180o rotation. Therefore, the model of two subduction zones proposed by some previous studies may better explain the complex structure below the Banda arc.

Cardwell and Isacks[4] interpret that the subduction zone to the north of the Banda Sea is not a continuation of the one along the southern and eastern parts of the arc. The southern arm has been rotated 90° and stopped at the easternmost part of the arc; while the northern arm has resulted from the counter clockwise rotation of the Bird's Head combined with the westward movement of the Pacific.[5] Fault plane solutions by Cardwell and Isacks[4] depict that the slab beneath the eastern Banda arc that is contorted has undergone a lateral compression, which may be due to the bending; while away from the contorted part of the slab the stresses are oriented more in the downdip configuration.[6] Such lateral bending stresses are also observed in the gently curved Mariana and southern New Hebrides arcs.[29] All of these observations support the explanation of the two slabs model. However, the weakness is that there is little evidence of the subduction from the north.[11]

The debate whether the Banda arc has been rotated 180° or 90° remains challenging. Our inversions alone cannot resolve such detail. However, from the layer anomaly maps for the upper mantle structure shown in Figure 3 (from 90 to 190 km), our new tomograms clearly depict the twisting of the slab nearly parallel to the present-day curved Banda arc. While the two contrasting explanations are still unresolved, recently Spakman and Hall[11] have proposed the model of a single slab rolling back toward the Banda embayment based on seismic tomography and plate reconstruction. If a Jurassic embayment that once existed within the Australian plate is true as shown by Hall,[30] the model of a single slab rolling back toward the embayment as proposed by Spakman and Hall[11] may represent the best explanation of how the spoon-shaped feature beneath the Banda arc has been formed. They suggest that the westward component of crustal flow north and northeast of the northern arm of the Banda arc resulted from the coupling between the Australian and Pacific plates and the strong reduction of Australian northward motion resulting from mantle resistance to slab transport.

For further investigation of the complex structure below the Banda arc we show seismicity maps (Figure 5) in detail at the depth intervals used for the vertical parameterization in the tomographic imaging. The first layer of the seismicity map representing the crustal structure does not show clearly a continuous seismicity bend beneath the southern and northern arms of the Banda arc. Instead, there is a clear seismicity gap underneath the eastern Banda arc, decoupling the laterally continuous seismicity zones beneath the Aru and Seram troughs. These two seismicity zones appear to be continuous at deeper depths, i.e., down to 490 km depth, due to the convergent directions of descending lithospheres beneath the Aru and Seram troughs i.e. N-NW and SW, respectively, both toward the Banda Sea. We do not observe seismicity associated with the descending slab beneath the Seram trough at depth intervals below 490 km. This suggests that the deep subduction that represents the major subduction is due to the continent-arc convergence beneath the southern arm of the Banda arc. The pattern of seismicity and its position in the depth intervals (660-490 km), (490-220 km), (220-70 km), and (70-0 km) are well associated with the proposed locations of the trench at 15, 7, 4 and 0 Myr ago, respectively.[30] Thus the inference from the seismicity maps strongly supports the model of a single slab rolling back as proposed by Spakman and Hall.[11]

As detailed structural features are often well defined by carefully relocated events, for future work we will focus on refining locations by following the approach introduced by Pesicek *et al.*,[31] i.e., to improve upon the comprehensive EHB catalog of seismicity used in this study by applying a multiple-event double-difference (DD) relocation technique to teleseismically recorded events with a 3-D velocity model at a

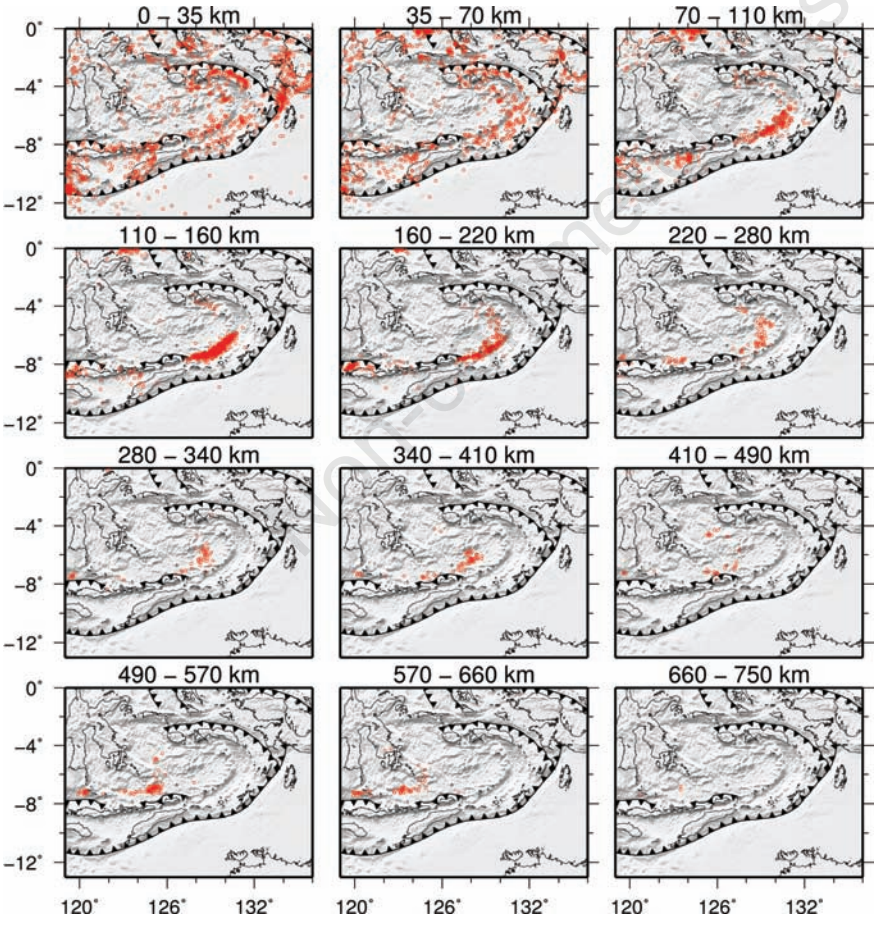

Figure 5. Distribution of EHB earthquakes (1964-2007) plotted as maps at the depth intervals used for the vertical parameterization in the tomographic imaging. Notice the intense seismic activities in the depth interval of 0-70 km below the Seram trough and 70-220 km below the Aru trough.

finer scale. To do this, we will incorporate the new local data set from the Meteorological, Climatological and Geophysical Agency of Indonesia to increase data coverage and provide further assessment of the complex lithospheric structure beneath the Banda arc.

References

1. Katili JA. Volcanism and plate tectonics in the Indonesian Island arcs. Tectonophysics 1975;26:165-88.
2. Hatherton T, Dickinson WR. The relationship between andesitic volcanism and seismicity in Indonesia, the Lesser Antiles, and other island arc. J Geophys Res 1969;74:5301-10.
3. Fitch TJ, Hamilton W. Reply. J Geophy Res 1974;79:4982-85.
4. Cardwell RK, Isacks BL. Geometry of the subducted lithosphere beneath the Banda Sea in eastern Indonesia from seismicity and fault plane solutions. J Geophy Res 1978; 83:2825-38.
5. McCaffrey R. Active tectonics of the Sunda and Banda arcs. J Geophys Res 1988;93:15163-82.
6. Matejkova R, Spicak A, Hanus V, Vanek J. A two-slab model of the Banda arc, Southeast Asia. Southeast Asian Gateway Evolution Conference (abstract). Royal Holloway University of London, United Kingdom; 2009.
7. Engdahl ER, van der Hilst RD, Buland R. Global teleseismic earthquake relocation with improved travel times and procedures for depth determination. Bull Seism Soc Am 1998;88:722-43.
8. Puspito NT, Yamanaka Y, Miyatake T, et al. Three-dimensional P-wave velocity structure beneath the Indonesian region. Tectonophysics 1993;220:175-92.
9. Widiyantoro S, van der Hilst RD. Mantle structure beneath Indonesia inferred from high-resolution tomographic imaging. Geophys J Int 1997;130:167-82.
10. Bijwaard H, Spakman W, Engdahl ER. Closing the gap between regional and global traveltime tomography. J Geophy Res 1998;103:30055-78.
11. Spakman W, Hall R. Surface deformation and slab-mantle interaction during Banda arc subduction rollback. Nature Geosci 2010;3:562-6.
12. Pesicek JD, Thurber CH, Widiyantoro S, et al. Sharpening the Tomographic Image of the Subducting Slab below Sumatra, the Andaman Islands, and Burma. Geophys J Int 2010;182:433-53.
13. Fukao Y, Obayashi M, Inoue H, Nenbai M. Subducting slabs stagnant in the mantle transition zone. J Geophys Res 1992;97:4809-22.
14. Widiyantoro S, van der Hilst RD. Structure and evolution of lithospheric slab beneath the Sunda Arc, Indonesia. Science 1996;271:1566-70.
15. Paige C, Saunders MA. LSQR: An algorithm for sparse linear equations and least squares problems. ACM Trans Math Soft 1982;8:195-209.
16. Nolet G. Seismic wave propagation and seismic tomography. In: Nolet G, editor. Seismic Tomography. Reidel, Dordrecht, Netherlands; 1987. pp. 1-23.
17. Bijwaard H, Spakman W. Non-linear global P-wave tomography by iterated linearized inversion. Geophys J Int 2000;141:71-82.
18. Widiyantoro S, Gorbatov A, Kennett BLN, Fukao Y. Improving global shear wave traveltime tomography using three-dimensional ray tracing and iterative inversion. Geophys J Int 2000;141:747-58.
19. Koketsu K, Sekine S. Pseudo-bending method for three-dimensional seismic ray tracing in a spherical earth with discontinuities. Geophys J Int 1998;132:339-46.
20. Um J, Thurber CH. A fast algorithm for two-point seismic ray tracing. Bull Seism Soc Am 1987;77:972-86.
21. Bassin C, Laske G, Masters G. The current limits of resolution for surface wave tomography in North America. EOS Trans Am Geophys Union 2000;81:F897.
22. Weidle C, Widiyantoro S, CALIXTO Working Group. Improving depth resolution of teleseismic tomography by simultaneous inversion of teleseismic and global P-wave travel time data – Application to the Vrancea region in southeastern Europe. Geophys J Int 2005;162:811-23.
23. Kennett BLN, Engdahl ER, Buland R. Constraints on seismic velocities in the Earth from traveltimes. Geophys J Int 1995;122:108-4.
24. Aster RA, Borchers B, Thurber C. Parameter Estimation and Inverse Problems. Amsterdam: Elsevier/Academic Press; 2005. pp. 296.
25. Engdahl ER, Villasenor A, DeShon HR, Thurber CH. Teleseismic Relocation and assessment of seismicity (1918-2005) in the region of the 2004 Mw 9.0 Sumatra-Andaman and 2005 Mw 8.6 Nias Island great earthquakes. Bull Seism Soc Am 2007;97:S43-61.
26. Fichtner A, De Wit N, van Bergen M. Subduction of continental lithosphere in the Banda Sea region: Combining evidence from full waveform tomography and isotope ratios. Earth Planet Sci Lett 2010;297:405-12.
27. Pesicek JD, Thurber CH, Widiyantoro S, et al. Complex slab subduction beneath northern Sumatra. Geophys Res Lett 2008;35:L20303.
28. Puspito NT, Shimazaki K. Mantle structure and seismotectonics of the Sunda and Banda arcs. Tectonophysics 1995;251:215-28.
29. Isacks B, Molnar P. Distribution of stress in the descending lithosphere from a global survey of focal mechanism solutions of mantle earthquakes. Rev Geophys Space Phys 1971;9:103-74.
30. Hall R. Cenozoic geological and plate tectonic evolution of SE Asia and the SW Pacific: computer-based reconstructions, model and animations. J Asian Earth Sci 2002;20:353-431.
31. Pesicek JD, Thurber CH, Zhang H, et al. Teleseismic double-difference relocation of earthquakes along the Sumatra-Andaman subduction zone using a 3-D model. J Geophys Res 2010;115:B103003.